Aquatic Mammals 2018, *44*(5), 506-518, DOI 10.1578/AM.44.5.2018.506

Lens Lipidomes Among Phocidae and Odobenidae

Raphaela Stimmelmayr[1,2] and Douglas Borchman[3]

[1]*North Slope Borough Department of Wildlife Management, PO Box 69, Barrow, AK 99723, USA*
[2]*Institute of Arctic Biology, University of Alaska, Fairbanks, AK, USA*
[3]*Department of Ophthalmology and Visual Sciences, University of Louisville, Kentucky Lions Eye Center, 301 E. Muhammad Ali Boulevard, Louisville, KY 40202, USA*
E-mail: borchman@louisville.edu

Abstract

Why do seals develop cataracts after living 40 years, rats after 2 years, and humans after 70 years, while whales do not develop cataracts even after 100 years of age? To address that question, lenses from pinnipeds—walrus, spotted seals, ringed seals, bearded seals, and a ribbon seal—were studied. The cholesterol and phospholipid content of the lenses were measured using ^{1}H and ^{31}P-NMR spectroscopy, respectively. Lens lipid structure was measured using FTIR spectroscopy. We found that in Phocidae, similar to various terrestrial species, lifespan is related to lens sphingolipid, and lens sphingolipid is related to lens membrane order and cholesterol. Shifting lens lipid composition toward increased levels of sphingolipids has been proposed as an adaptive evolutionary molecular mechanism to limit reactive oxygen species lens damage (oxidative stress) and, thus, age-related cataract formation. Additional comparative studies of lens lipid composition of pinnipeds across taxa with various foraging and diving strategies are needed to further explore and test underlying assumptions for the observed divergent sphingolipid content between Phocidae and Odobenidae. While the causes of the lens compositional differences between Phocidae and Odobenidae remain undetermined, our study provides novel physiological data on lens lipid composition in marine mammals and largely complements lens lipid compositional findings in terrestrial and other aquatic species that demonstrate a linkage between lifespan, sphingolipids, and cataracts.

Key Words: pinnipeds, seals, walruses, cataract, lens, lifespan, lipids

Introduction

The vertebrate eye lens is a highly specialized avascular clear tissue. Across mammalian species, eye lenses not only differ in weight and shape but also show remarkable differences in lens lipid composition and order. Specifically, lens lipidome analysis in species with a maximum lifespan ranging between 30 to 150 y has shown that lens sphingolipid levels correlate with lifespan and age-related cataract formation (Borchman et al., 2004, 2017; Borchman & Yappert, 2010). Lens lipid composition and its correlation to lifespan and age-related cataract formation has not been studied in diving mammals with the exception of the bowhead whale (*Balaena mysticetus*), a long-lived, ice-associated baleen whale (George et al., 1999; Zeh et al., 2013; Borchman et al., 2017).

Sphingolipids are a class of complex lipid moieties that play an important role in cell signaling in terrestrial mammals (Dickson, 1998). Shifting lens lipid composition toward increased levels of sphingolipids has been proposed as an adaptive evolutionary molecular mechanism to limit reactive oxygen species (ROS) lens damage (oxidative stress) and thus age-related cataract formation (Borchman et al., 2004, 2017). Lens membranes with a high content of saturated sphingolipids are less susceptible to oxidation because there is relatively less oxygen in these ordered bilayers, as well as fewer double bonds to become oxidized (Pamplona et al., 1998, 1999a, 1999b; Herrero et al., 2001; Portero-Otin et al., 2001; Oborina & Yappert, 2003; Borchman & Yappert, 2010). Furthermore, lens lipid hydrocarbon order is directly related to the sphingolipid content and indirectly related to the phosphatidylcholine content of the lenses of many animals. Thus, a high-saturated sphingolipid content and increased headgroup interactions cause the lipid hydrocarbon chain region to become more ordered (Ferguson-Yankey et al., 2000; Talbot et al., 2000). As a consequence of higher lipid order, membranes may be less susceptible to oxidative damage because oxygen is five times more soluble in lipid membranes than it is in the aqueous (Power & Stegall, 1970; Kimmich & Peters, 1975; Kimmich et al., 1981; Subczynski & Hyde, 1983; Vanderkooi et al., 1990; Smotkin et al., 1991). In addition,

oxygen is five to 10 times more soluble in fluid membranes (Smotkin et al., 1991), such as membranes low in sphingolipids, than it is in the aqueous. Lipidome analysis of cataracterous lenses has shown changes in lipid composition and membrane structure that contribute to lens opacity (Borchman et al., 1993, 1996; Huang et al., 2005; Borchman & Yappert, 2010).

Lens sphingolipid levels in bowhead whales exceed levels observed in other long-lived species, including humans, and cataracts are not known to occur in this species (Philo et al., 1993; Stimmelmayr, 2015). Northern pinniped species, including ringed seals (*Phoca hispida*), bearded seals (*Erignathus barbatus*), spotted seals (*Phoca largha*), ribbon seals (*Phoca fasciata*), and Pacific walrus (*Odobenus rosmarus*), have relatively long lifespans ranging between 30 to 45 y (McLaren, 1958; Fay, 1982; Boveng et al., 2009; Cameron et al., 2010). The incidence of cataract formation in ice seals is unknown, but nuclear cataracts have been observed in these species (Stimmelmayr, unpub. data, 2012-2015). Cataracts are well-documented eye diseases occurring in diving mammals (e.g., otarids, Odobenidae, and small cetaceans) under human care, and extended lifespan among other risk factors (e.g., diet, genetics, trauma, and environmental and husbandry factors) have been implicated in cataract formation in captive aquatic species (Hubbard, 1970; Greenwood, 1985; Coolitz et al., 2010).

The aim of the present study was to analyze lens lipid composition, lipid order, and changes in lens cholesterol content of four long-lived northern pinnipeds from two different taxa (Phocidae and Odobenidae) thereby significantly expanding the representation of Arctic and diving mammals in general within the comparative field of lens lipid analysis. We furthermore explore and discuss phylogeny, diet, and diving behavior as possible explanatory variables in the observed differences in lens lipid parameters from this study.

Methods

The methods used in this study were identical to those used to study whale lenses (Borchman et al., 2017).

Globe Enucleation, Lens Dissection, and Lipid Extraction

The harvest of marine mammals for subsistence purposes by Alaskan natives is exempted under the Marine Mammal Protection Act of 1972 (MMPA), Section 1379. Eye globes were opportunistically collected from subsistence harvested ringed, bearded, spotted, and ribbon seals and Pacific walrus during June and July 2011 to 2014 in Utqiagvik (71.2906° N, 156.7886° W) and Wainwright (70.6369° N, 160.0383° W), Alaska. Animals were aged according to body size and dental development and classified as young of the year (< 1 y), subadult (1 to 5 y), and adult (> 6 y) (McLaren, 1958; Fay, 1982; Boveng et al., 2009; Cameron et al., 2010). Eye globes were enucleated using scissors and stored whole frozen in Whirl-Paks® at -20° C until analyzed. From time of death to sample collection took on average 5 to 10 h. Marine mammal tissue samples used in this study were collected under National Marine Fisheries Service Permits 17350-00 and 17350-01 and U.S. Fish and Wildlife Service Permit MA134907-1.

Previously frozen pinniped lenses were removed from the globe by an anterior approach. The iris and ciliary body were carefully removed from the lens by cutting the zonules when present with curved micro-scissors. Lenses were each extracted using a monophasic methanol extraction procedure that gave the highest yield of lens phospholipid compared to other extraction protocols (Byrdwell et al., 2002). Lenses were each added to 5 mL of methanol (Sigma-Aldrich, St. Louis MO, USA) in a 25-mL glass scintillation vial (Fisher Scientific, Pittsburgh PA, USA) and chopped using a Teflon™ coated spatula. Argon gas (Analyzed, Ultra-Pure; Welders Supply, Louisville, KY, USA) was bubbled into the methanol/lens mixture for 2 min to remove oxygen. The vial was sonicated in an ultrasonic bath (Model 1510; Branson Ultrasonics, Danbury, CT, USA) for 10 min. The mixture was centrifuged for 10 min at 10,000 × g. The supernatant was decanted and dried with a stream of Argon gas. Methanol (5 mL) was added to the pellet, and the procedure above from the bubbling of Argon gas on was repeated two times with the supernatant from the centrifugation step added to the supernatant(s) from the previous steps and dried with a stream of Argon gas. To ensure all methanol was removed from the sample, it was dried further in a lyophilizer set at 29 torr and a condenser temperature < -50ºC (Freeze Dryer 3; Labconco, Kansas City, MO, USA) for 1 h to remove all solvent. $CDCl_3$ (1 mL; Sigma-Aldrich) was added to the dried lipid. The vial was sonicated in an ultrasonic bath (Model 1510; Branson Ultrasonics) for 10 min, and the mixture was placed into a 9-mm microvial with a Teflon™ cap (Microliter Analytical Supplies, Suwanee, GA, USA) to which Argon gas was added. Samples were stored for no more than 24 h at -20ºC.

Cholesterol to Phospholipid Ratio Analysis Using H-NMR

Half (500 µL) of the lens lipid-$CDCl_3$ extract was transferred from the microvial to an NMR tube using a glass pipet. Spectral data were acquired using a Varian VNMRS 700 MHz NMR

spectrometer (Varian, Lexington, MA, USA) equipped with a 5-mm $^{1}H\{^{13}C/^{15}N\}^{13}C$ enhanced PFG cold probe (Palo Alto, CA, USA). Spectra were acquired with a minimum of 250 scans, 45º pulse width, and a relaxation delay of 1.000 s. All spectra were obtained at 25ºC. Spectra were processed, and integration of spectral bands was performed with *GRAMS/386* software (Galactic Industries, Salem, NH, USA). Cholesterol to phospholipid molar ratios were calculated as discussed in the "Results" section.

Measurement of Phospholipid Composition Using ^{31}P-NMR

A methanol/0.2M Cs-EDTA (4:1) reagent (Meneses & Glonek, 1988) was added (250 µL) to the sample used for H-NMR spectroscopy and homogenized with the use of a temperature-controlled ultrasonic bath at 40°C for 10 min. ^{31}P-NMR spectra traces were measured using a Varian Inova-400 spectrometer. The parameters to perform the acquisitions were similar to those described previously (Estrada et al., 2010). Briefly, a spectral width of 2,024.7 Hz (sweep width δ = 10 ppm), 60° pulse, 4,000 data points, 1.0 s delay time, 0.711 s acquisition time, and proton decoupling (WALTZ) at 500.16 MHz were used. A line broadening of 3.0 Hz and phase correction were used to process the spectra. Chemical shifts were referenced to internal or added bovine brain sphingomyelin (Sigma-Aldrich) resonance at δ = -0.09 ppm. Spectra were processed, and integration of spectral bands was performed with *GRAMS/386* software.

Measurement of Lipid Phase Transitions Using FTIR Spectroscopy.

The 500 µL of sample not used for NMR analysis was applied to an AgCl infrared window. The solvent was evaporated under a stream of Argon gas, and the window was placed in a lyophilizer for 4 h to remove all traces of solvent. Infrared spectra were measured using a Fourier transform infrared spectrometer (Nicolet 5000 Magna Series; Thermo Fisher Scientific, Inc., Waltham, MA, USA). Lipid on the AgCl window was placed in a temperature-controlled infrared cell. The cell was jacketed by an insulated water coil connected to a circulating water bath (Model R-134A; Neslab Instruments, Newton, NH, USA). The sample temperature was measured and controlled by a thermistor touching the sample cell window. The water bath unit was programmed to measure the temperature at the thermistor and to adjust the bath temperature so that the sample temperature could be set to the desired value. The rate of heating or cooling (1°C/15 min) at the sample was also adjusted by the water bath unit. Temperatures were maintained within ± 0.01°C. Exactly 100 interferograms were recorded and averaged. Spectral resolution was set to 1.0 cm^{-1}. Infrared data analysis was then performed using *GRAMS/386* software. The frequency of the symmetric CH_2 stretching band near 2,850 cm^{-1} ($\tilde{\nu}_{sym}$) was used to estimate the content of *trans* and *gauche* rotamers in the hydrocarbon chains. $\tilde{\nu}_{sym}$ was calculated by first baseline leveling the OH-CH stretching region between 3,500 and 2,700 cm^{-1}. The center of mass of the CH symmetric stretching band was calculated by integrating the top 10% of the intensity of the band. The baseline for integrating the top 10% of the intensity of the band was parallel to the OH-CH region baseline. The change in $\tilde{\nu}_{sym}$ vs temperature was used to characterize lipid phase transitions as described previously (Borchman et al., 2007). Since rotamers are either in *trans* or *gauche* conformations, phase transitions were fit to a two-state sigmoidal equation using *SigmaPlot 10* software (Systat Software, Inc., Chicago, IL, USA):

Equation 1:

$$\tilde{\nu}_{sym} = (\tilde{\nu}_{sym})_{minimum} + ((\tilde{\nu}_{sym})_{maximum} - (\tilde{\nu}_{sym})_{minimum})/(1+ (temperature/Tc)^{hillslope})$$

$\tilde{\nu}_{sym}$ is the frequency of the symmetric CH_2 stretching band near 2,850 cm^{-1}. Tc is the phase transition temperature.

Lipid order at 25° and 33.4°C was calculated by extrapolating the $\tilde{\nu}_{sym}$ at 25° and 33.4°C from the fit of the phase transition and then converting $\tilde{\nu}_{sym}$ to the percentage of *trans* rotamers, a measure of lipid conformational order (Borchman et al., 2007). The data for percentage of *trans* rotamer were used to calculate the phase-transition enthalpy and entropy from the slopes of Arrhenius plots (Borchman et al., 2007).

Results

A total of 13 pinnipeds, three specimens per species with the exception of the ribbon seal where only one specimen was available, were included in this study. Age distribution was three young of the year (< 1 y), three subadults (1 ≤ 5 y), and seven adults (≥ 6 y). Sex distribution was four males, eight females, and one seal of undetermined sex. Lens diameter (cm) among Phocidae ranged between 0.8 to 1.7 cm. Minimum average lens weight (g) was 0.8 ± 0.7 for bearded seals, and maximum average lens weight (g) was 2.4 ± 0.8 for ringed seals. Lens diameter (cm) for Pacific walrus could not be determined. Average lens weight (g) for Odobenidae was 0.3 ± 0.2. The weights and size of the spherical lenses are presented in Table 1.

Table 1. Demographics and phase transition parameters of lens lipids

	Lens properties		Phase transition parameters							
Sample	Diameter range (cm)	Weight (g)	Min (cm^{-1})	Max (cm^{-1})	Tc (ºC)	Coop	Order 25.8ºC (% trans)	Order 33.4ºC (% trans)	ΔH (Kcal/ mole)	ΔS (Kcal/mole/ degree)
Walrus	n.d.	0.3 ± 0.2	2,851.2 ± 0.3	2,852.2 ± 0.3	40 ± 13	1.7 ± 1.9	50 ± 4	46 ± 4	31.9 ± 0.3	0.102 ± 0.001
Ringed seal	1.3-1.7	2.4 ± 0.8	2,851.2 ± 0.3	2,853.0 ± 1	40 ± 14	3 ± 2	50 ± 4	46 ± 4	31.7 ± 0.3	0.101 ± 0.001
Bearded seal	0.8-1.4	0.8 ± 0.7	2,851.9 ± 0.2	2,854.3 ± 0.3	32 ± 3	3.9 ± 1.6	38 ± 3	30 ± 3	74.1 ± 0.8	0.243 ± 0.003
Ribbon seal	1.6	3	2,851.04 ± 0.06	n.d.	37 ± 2	6.4 ± 1.9	57.00 ± 0.09	52.5 ± 0.9	34 ± 2	0.109 ± 0.005
Spotted seal	1.2-1.5	1.5 ± 0.5	2,850.9 ± 0.1	2,854.3 ± 1	57 ± 24	2 ± 1	56 ± 1	53 ± 1	20.8 ± 0.3	0.063 ± 0.001

Notes: Average values ± Standard Error of the mean. Min = minimum symmetric CH_2 stretching band frequency, Max = maximum symmetric CH_2 stretching band frequency, Tc = phase transition temperature, Coop = relative cooperativity of the phase transition, ΔH = change in enthalpy of the transition, ΔS = change in entropy of the phase transition, and n.d. = not detected.

NMR Spectroscopy

^{31}P-NMR was used to quantify pinniped lens phospholipid composition (Figure 1). The sphingolipid composition of walrus lenses was greater, 84 ± 3%, compared with 49 ± 3% for seals (Table 2). The phosphatidylcholine composition of walrus lenses was less, 8 ± 1%, compared with 21 ± 3% for seals (Table 2). We were unable to obtain a good ^{31}P-NMR spectrum for the ribbon seal lens. Samples were spiked with bovine sphingomyelin to confirm the position of the resonances for sphingomyelin (-0.090 ppm) and dihydrosphingomyelin (0.117 ppm) (Estrada et al., 2010).

Cholesterol was quantitated from the H-NMR spectra of the lens lipid extracts. Phospholipid was quantified from the amide NH resonances near 6.81, 6.22, and 5.88 ppm (Figure 2a) assigned to hydrated and partially hydrated sphingolipid, respectively (Ferguson-Yankey et al., 2000; Talbot et al., 2000), the resonance near 3.48 ppm (Figure 2b) assigned to the choline head group N-CH_2 moiety, and the resonance near 3.9 assigned to the choline CH_3 resonance (Sparling et al., 1989; Ferguson-Yankey et al., 2000; Talbot et al., 2000). The assignments were reasonable as the resonances were in the correct positions. Furthermore, the measured average resonance ratios for the phospholipids NCH_2/amide-H, CH_3/amide-H_2, and NCH_2/CH_3 were 4 ± 0.6, 3.7 ± 0.3, and 1.3 ± 0.3, respectively, reasonably close to the expected intensity ratios of 3, 2, and 1.5, respectively.

Cholesterol was quantified from the CH_3 resonance near 0.67 ppm (Figure 2d) assigned to carbon 18 and the CH resonance near 1.83 ppm (Figure 2c) assigned to H1α, H2α, and H16α of the cholesterol molecule (Sawan et al., 1979; Muhr et al., 1996; Li et al., 1999). The assignments are reasonable as the resonances were in the correct position, and the measured (3 × CH)/CH_3 average intensity ratio was 0.98 ± 0.02, close to the expected intensity ratio of 1. At least four of the six combinations of cholesterol/phospholipid intensity ratios (two resonances for cholesterol and three resonances for phospholipid) were used to calculate the cholesterol to phospholipid molar ratio. The six combinations of cholesterol/phospholipid intensity ratios were used to calculate a cholesterol/phospholipid molar ratio with a relative SE of 5 ± 2% for each sample (Table 2). The largest percentage error was for the spotted seal (Table 2). Occasionally, resonances were not well-resolved, resulting in a cholesterol/phospholipid molar ratio greater than two SD units from the mean and were therefore not used in the calculation.

Infrared Spectroscopy

Infrared spectroscopy was used to measure lipid-lipid interactions and the composition of lens lipid suspensions from pinnipeds. The CH_2 stretching and bending bands were predominant in the infrared spectra of lipids due to the large number of CH_2 groups in their hydrocarbon chains (Figure 3). Tentative infrared band assignments are listed in Table 3. Note that the intensity of the carbonyl band near 1,740 cm^{-1} is very small compared to the intensity of the amide band near 1,650 cm^{-1} and CH_2 bending band near 1,470 cm^{-1}, which supports the large percentage of ether and amide linked hydrocarbon chains measured by ^{31}P-NMR (Figure 3). The CH stretching region

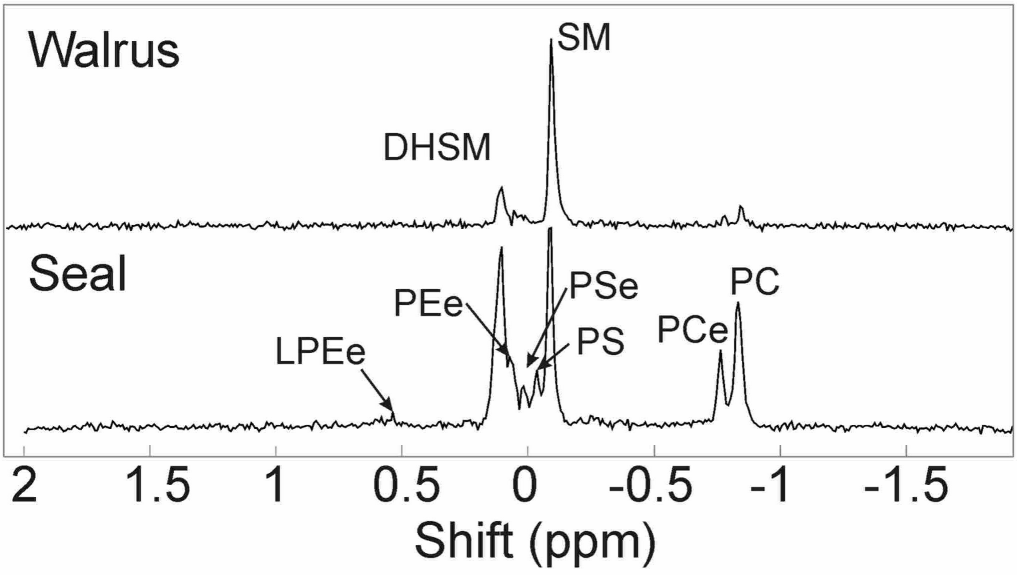

Figure 1. Average ^{31}P-NMR spectra of phospholipids extracted from seal and walrus lenses. DHSM = dihydrosphingomyelin, PEe = phosphatidylethanolamine ether, PS = phosphatidylserine, PSe = phosphatidylserine ether, PCe = phosphatidylcholine ether, PC = phosphatidylcholine, and SM = sphingomyelin.

Table 2. Pinniped demographics and lens lipid composition

	Mole % of total phospholipid								C:PL mole: mole
Sample	LPEe/PGe	DHSM	PEe	PSe	PS	SM	PCe	PC	
Walrus	1 ± 1	16 ± 3	1 ± 1	4 ± 2	n.d.	68 ± 2	1 ± 1	7 ± 2	7.0 ± 0.2
Ringed seal	1 ± 1	25 ± 4	13 ± 6	6 ± 3	4 ± 4	25 ± 5	9 ± 1	18 ± 6	2.9 ± 0.1
Bearded seal	n.d.	22 ± 11	2 ± 2	16 ± 11	6 ± 2	24 ± 2	8.3 ± 0.4	22 ± 2	6.5 ± 0.2
Spotted seal	1 ± 1	28 ± 6	10 ± 6	7 ± 2	n.d.	23 ± 2	8 ± 5	23 ± 8	4.3 ± 0.4
Ribbon seal	No ^{31}P-NMR spectrum								3.0 ± 1.0

Notes: LPEe/PGe = lyso phosphatidylethanolamine either/phosphatidylglycerol ether, DHSM = dihydrosphingomyelin, PEe = phosphatidylethanolamine ether, PSe = phosphatidylserine ether, PS = phosphatidylserine, SM = sphingomyelin, PCe = phosphatidylcholine ether, PC = phosphatidylcholine, C = cholesterol, PL = phospholipid, and n.d. = not detected. Data are the average ± SE for three samples, except for the ribbon seal with an *n* of 1.

near 2,900 cm^{-1} is composed of six major bands (Borchman et al., 2007). In this study, we used the $\tilde{\nu}_{sym}$ near 2,850 cm^{-1} to estimate the *trans* to *gauche* rotamer content of the hydrocarbon chains (Figure 3). The $\tilde{\nu}_{sym}$ increased with an increase in temperature and an increase in the number of *gauche* rotamers, concurrent with a decrease in intensity (Kóta et al., 1999; Figure 4). Lipid phase transitions were quantified by fitting them to a four-parameter, two-state sigmoidal equation as described by Borchman et al. (2007). The four parameters fitted were the minimum and maximum $\tilde{\nu}_{sym}$ in the phase transition that correspond to the most ordered and disordered states, respectively; the transition temperature at which half of the lipid molecules underwent a phase change; and the relative cooperativity. The broader the phase transition, the smaller the absolute value of the cooperativity. Cooperativity describes how the order of a lipid influences that of neighboring lipids. The four phase-transition parameters necessary for defining the phase transition and other parameters calculated from the defining parameters are listed in Table 1.

Lipid order was measured presumably close to the temperature of the pinniped eye, 33.4°C, by extrapolating the $\tilde{\nu}_{sym}$ at 33.4°C from the fit of the phase transition and then converting $\tilde{\nu}_{sym}$

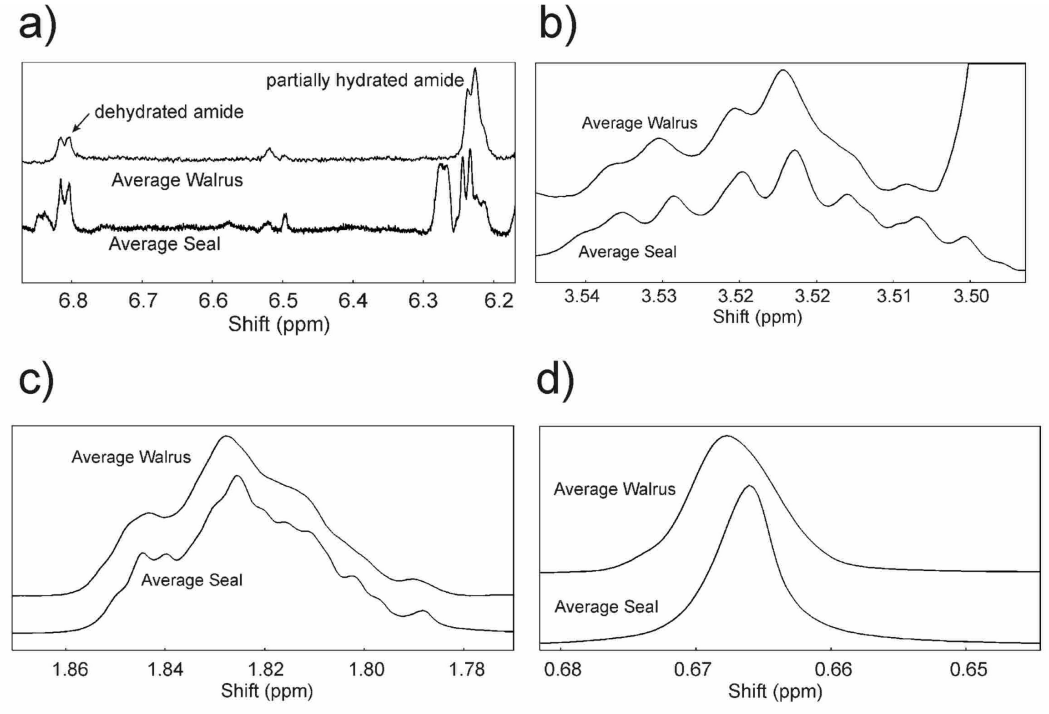

Figure 2. H-NMR spectra of lipids extracted from pinniped lenses. The spectra were used to quantify the molar cholesterol/phospholipid ratios of the extracts. Phospholipid was quantified from the amide NH resonances near 6.81 and 6.22 ppm (a) assigned to hydrated and partially hydrated sphingolipid, respectively, and the resonance near 3.48 ppm (b) assigned to the choline head group N-CH_2 moiety. Cholesterol was quantified from the CH_3 resonance near 0.67 ppm (c) assigned to carbon 18 and the CH resonance near 1.83 ppm (d) assigned to carbons 2, 16, and 24 of the cholesterol molecule.

to the percentage of *trans* rotamers (Borchman et al., 2007; Table 1). Lipid order at 25°C was also calculated (Table 1) since the temperature of pinniped lenses exposed to extremely low Arctic temperatures could be lower than that for humans.

Correlations

There was a linear correlation between the percentage of lens sphingolipid and lens lipid hydrocarbon chain order measured at 34.8ºC ($r = 0.89$, $n = 15$, $p < 0.01$; Figure 5a) until about 60% sphingolipid, above which there was little change in the hydrocarbon chain order. The values for the pinniped lenses measured in this study (Figure 5a) fit well with those measured in other studies. The percentage of lens sphingolipid correlated with lens lipid phase transition temperature ($r = 0.49$, $n = 13$, $p < 0.01$; Figure 5b). Hydrocarbon chain order and the phase transition temperature for lens lipids were linearly related ($p < 0.1$). The percentage of pinniped lens sphingolipid measured in this study was statistically correlated with the percentage of lens sphingolipid and expected maximal lifespan measured in other studies (sigmoidal fit: $r = 0.89$, $n = 41$, $p < 0.01$; Figure 6a). The percentage of lens phosphatidylcholine fit well in the correlation between the percentage of lens sphingolipid and expected maximal lifespan measured from other studies (sigmoidal fit: $r = 0.91$, $n = 32$, $p < 0.01$; Figure 6b). The percentage of walrus lens sphingolipid deviated the most from the curves. The percentage of cholesterol in the phocid lens fit well in the correlation between the

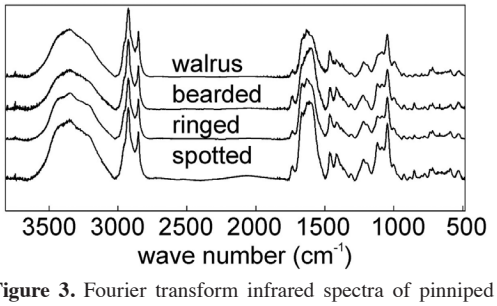

Figure 3. Fourier transform infrared spectra of pinniped lens lipids

Table 3. Tentative infrared band assignments

Lipid band (cm^{-1})	Tentative band assignment
695-738	CH_2, rock
918	OH carboxylic acid
960	C-N-C
1,043	C-O, ester stretch
1,067	Symmetric stretch, PO_2^- groups
1,172	C-O
1,245	C-O
1,272	Asymmetric stretch, PO_2^- groups
1,349	CH_2 wagging progression
1,366	CH_2 wagging progression
1,378	CH_2 wagging progression, C-H bend, CH_3 groups
1,408	Symmetric stretch, COO^- groups
1,469	CH_2 in plane bends
1,650	Conjugated dienes, amides
1,739	C = O, acyl linkage
2,950	Symmetric stretch, CH_2
2,924	Asymmetric stretch, CH_2 group
2,957	Asymmetric stretch, CH_3 groups
3,010	CH stretch, -HC = CH- moiety
3,208	OH stretch
3,348	OH stretch
3,453	OH stretch, O-O-H stretch

percentage of cholesterol and sphingolipid (r = 0.91, n = 20, p < 0.01; Figure 7).

Discussion

The major findings of this study were that in Phocidae, similar to various terrestrial species, lifespan is related to lens sphingolipid, and lens sphingolipid is related to lens membrane order and cholesterol (Borchman et al., 2004, 2017; Borchman & Yappert, 2010). The observed difference in lens sphingolipid composition between Phocidae and Odobenidae is intriguing.

With respect to lens sphingolipids content, the four ice-associated seal species group together, while the Pacific walrus grouped with the polar bear (*Ursus maritimus*) (Figure 6a). Both Pacific walrus and polar bear have a relatively small eye globe (globe diameter: Pacific walrus, 25 mm; polar bear, 18 mm) and lens (equatorial lens diameter: Pacific walrus, 11 mm; polar bear, 10 mm) in comparison to the other pinnipeds. For example, bearded and ringed seal globe diameters range from 34 to 45 mm (Stimmelmayr, unpub. data, 2018). The observed lens sphingolipids grouping is consistent with a pinniped diphyly view where Ursidae, Odobenidae, and Otaridae are sister taxa (Arnason et al., 2006; Higdon et al., 2007; Koretsky et al., 2016).

Sphingolipid levels measured in both Pacific walrus and polar bear are among the highest measured, only exceeded by the bowhead whale and the camel (*Camelus dromedarius*) (Borchman & Yappert, 2010). Camels are distant relatives to the hippo and whale clade (Gatesy et al., 2013; Wu et al., 2014) and, in contrast to bowhead whales, are known to develop cataracts (Dioli & Stimmelmayr, 1992; El-Tookhy & Tharwat, 2012). A thorough discussion of why these two taxa, superbly adapted to their environment (Xu et al., 2013; Seim et al., 2014; Yim et al., 2014), have comparable sphingolipid lens composition is beyond the scope of this article, but we speculate that in addition to lifespan, abiotic stress factors like oxygen availability for diving animals, salinity, and, in the case of camels, temperature, drive the need for high oxidative stress resistant lenses. Living in the desert, with limited water resources and high ambient temperature, camels are unique in their ability to withstand dehydration, salt loading, and elevated body temperature increases up to 40ºC (Schmidt-Nielsen et al., 1956, 1967; Wu et al., 2014). Oxidative

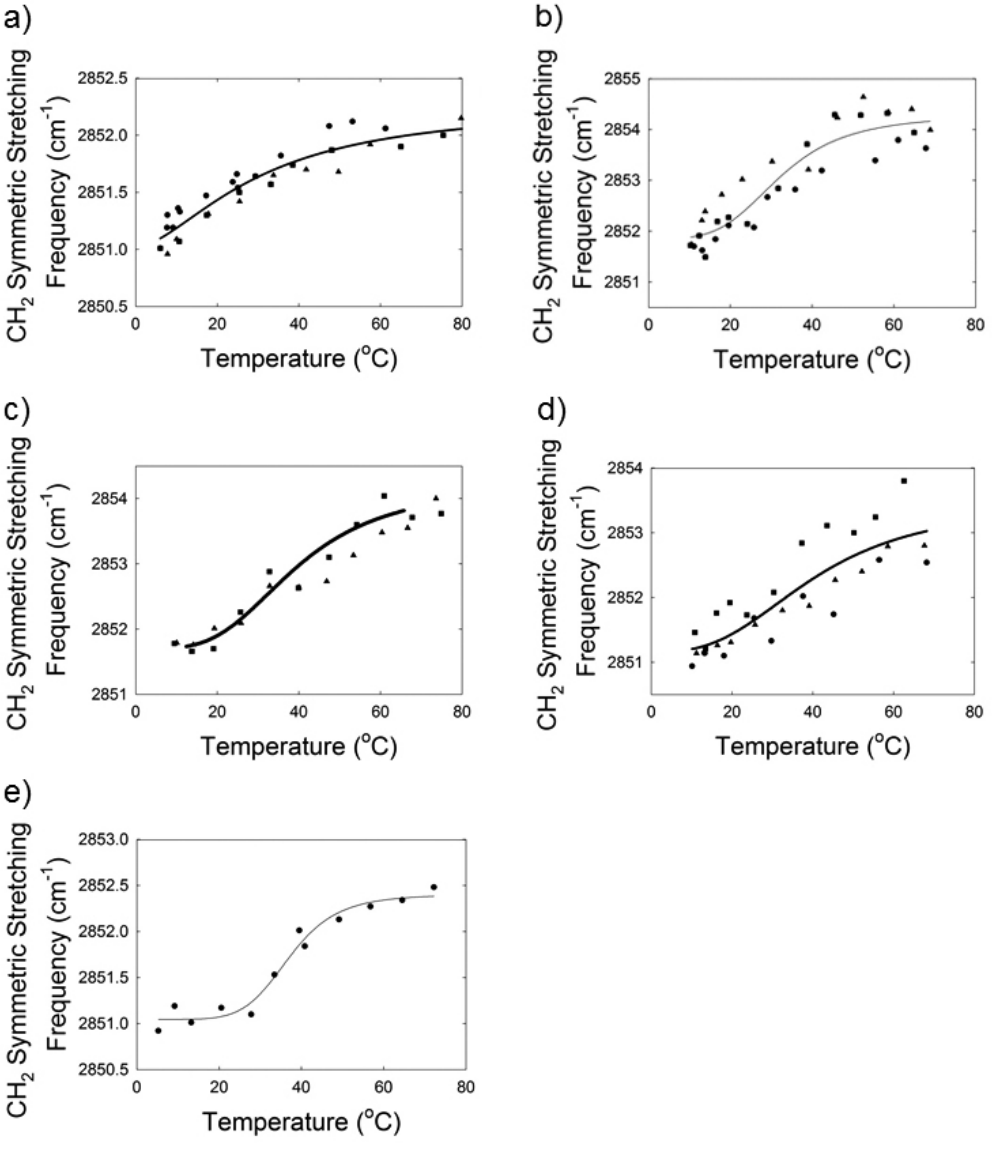

Figure 4. Lipid phase transition of aqueous suspensions of pinniped lens lipids: (a) walrus lens lipids, (b) bearded seal lens lipids, (c) spotted seal lens lipids, (d) ringed seal lens lipids, and (e) ribbon seal lens lipids. ▬ = curve fit of data to a four parameter sigmoidal curve. Data from the fit are presented in Table 1. An increase in the stretching frequency is associated with an increase in hydrocarbon chain gauche rotamers, disorder, and fluidity.

stress is inherent to these high energy processes, and increased ROS generation is associated with elevated body temperature (Davies, 1995; Brzezińska-Slebodzińska, 2001) and salt stress (Rivera-Ingraham et al., 2016; Rivera-Ingraham & Lignot, 2017). Similarly, hypoxemia is associated with increased ROS generation (Hermes-Lima et al., 2015). Thus, by living in the ocean, whales, like pinnipeds, must cope with ROS formation from osmoregulation and reduced oxygen availability (Ortiz, 2001; Cantú-Medellín et al., 2011; Vazquez-Medina et al., 2012) and the associated bio-energetic costs to maintain redox balance.

Given the diversity in life history (e.g., diet; diving strategy [shallow vs deep divers]), it is reasonable to speculate that they play a role, in

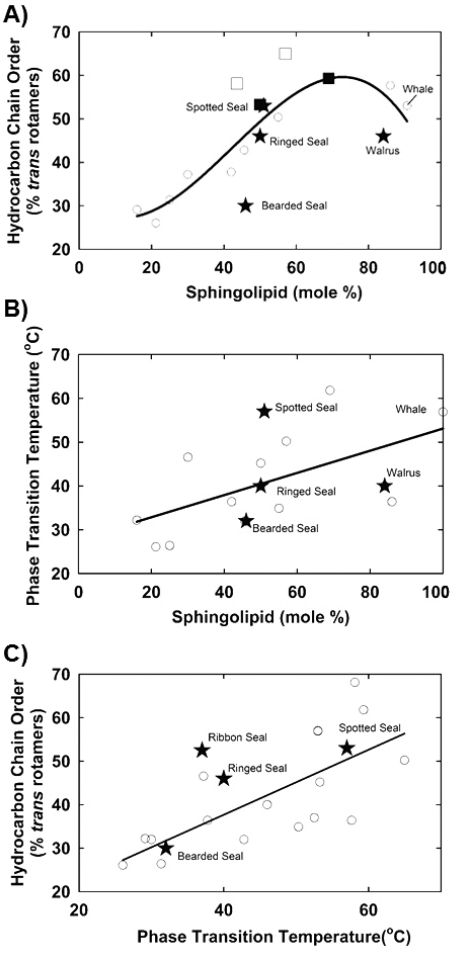

Figure 5. ★ = pinniped lipid phase transition parameters (Table 1) and phospholipid composition from Table 2; ● = data from Borchman et al. (2004, 2017); ■ = nuclear; and □ = cortical lens lipids from 25- and 70-y-old humans from Borchman et al. (1991, 1993, 1999).

addition to lifespan, in explaining the observed differences in the lens lipids of pinnipeds. Pacific walrus in both the Bering and Chukchi Seas feed on bivalves, gastropods, and polychaete worms (Fay, 1982; Sheffield & Grebmeier, 2009), while the four seal species forage on a combination of fish and various invertebrates (Frost & Lowry, 1980; Bluhm & Gradinger, 2008; Quakenbush et al., 2009; Crawford et al., 2015). However, despite the in general dynamic nature of cell membrane lipid composition in response to diet, nuclear lens cell membranes are somewhat unique with negligible lipid turnover rate, and evidence is lacking that diet per se modifies lens lipid composition (Nealon et al., 2008; Hughes et al., 2012, 2015).

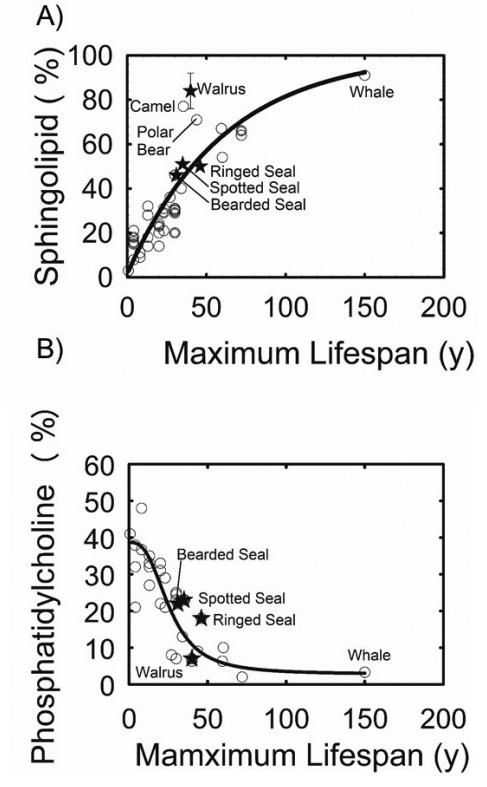

Figure 6. ★ = lifespan vs lipid phase transition parameters from Tables 1 and 2; and ● = data from Borchman et al. (2004, 2017).

Among the five seal species, ribbon seal are the deepest diving species (200 to 600 m), while dive behavior of bearded, ringed, and spotted seals are mostly confined to less than 200 m (Kelly & Wartzok, 1996; Gjertz et al., 2000; Boveng et al., 2009, 2013; Cameron et al., 2018). Pacific walruses are capable of deep dives, but, in general, they forage at around 80 m (Fay & Burns, 1988; Noren et al., 2015). Recent lipidome analysis provides evidence for differences in sphingolipid content of muscle cell membranes from pinnipeds with distinct diving capacities: the harbor (*Phoca vitulina*) and Weddell (*Leptonychotes weddellii*) seals (Young, 2013). Although suggestive that dive behavior may play a role in lipid composition, corroborating lens lipid composition data are lacking for these pinnipeds; thus, it remains to be seen if dive behavior indeed influences lens lipid composition.

While the causes of the lens composition differences between Phocidae and Odobenidae remain undetermined, our study provides novel physiological data on lens lipid composition in

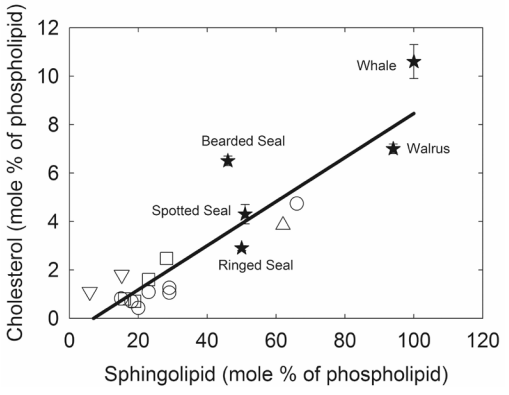

Figure 7. Relationship between the molar amounts of lens sphingolipid and cholesterol. ★ = pinnipeds from Table 1 and bowhead whale (100% SL) from Borchman et al. (2017); □ = calf lens cortex and nucleus (Broekhuyse et al., 1979), 2- to 6-y-old cow (Broekhuyse et al., 1979), and 1-y-old cow (Krause, 1935); ○ = cow, sheep, human, rat, mouse, pig, and chicken (Deeley et al., 2008); Δ = human lens (Borchman et al., 1989, 2005); and s = mice 10 and 45 d old (Andrews et al., 1991).

pinniped mammals and largely complements lens lipid composition findings in terrestrial and other aquatic species that demonstrate a linkage between lifespan, sphingolipids, and cataracts (Borchman et al., 2004, 2017; Borchman & Yappert, 2010). Additional comparative studies of lens lipid composition of pinnipeds across taxa with various foraging and diving strategies are needed to further explore and test underlying assumptions for the observed divergent sphingolipid content between Phocidae and Odobenidae.

Acknowledgments

We thank the hunters from Utqiagvik and Wainwright, Alaska, for their support of the North Slope Borough Department of Wildlife Management Ice Seal Bio-Monitoring Program. We thank Cyd Hanns, Greta Krafsur, Yosty Storm, Robert Sarren, and Billy Adams for technical assistance in the field. This study is funded by an unrestricted grant from Research to Prevent Blindness, Inc., New York, New York (GN151619B), and qualified outer continental shelf oil and gas revenues by a substantial grant (F12AF01265) from the Coastal Impact Assistance program, U.S. Fish and Wildlife Service, U.S. Department of the Interior, and the North Slope Borough.

Literature Cited

Andrews, J. S., Leonard-Martin, T., & Kador, P. F. (1984). Membrane lipid biosynthesis in the Philly mouse lens. I. The major phospholipid classes. *Current Eye Research*, *3*(2), 279-285. https://doi.org/10.3109/02713688408997210

Arnason, U., Gullberg, A., Janke, A., Kullberg, M., Lehman, N., Petrov, E. A., & Väinölä, R. (2006). Pinniped phylogeny and a new hypothesis for their origin and dispersal. *Molecular Phylogenetics and Evolution*, *41*(2), 345-354. https://doi.org/10.1016/j.ympev.2006.05.022

Barnes, S., & Quinlan, R. A. (2017). Small molecules, both dietary and endogenous, influence the onset of lens cataracts. *Experimental Eye Research*, *156*, 87-94. https://doi.org/10.1016/j.exer.2016.03.024

Bluhm, B. A., & Gradinger, R. (2008). Regional variability in food availability for Arctic marine mammals. *Ecological Applications*, *18*(2) Supplement, S77-S96. https://doi.org/10.1890/06-0562.1

Borchman, D., & Yappert, M. C. (2010). Lipids and the ocular lens. *Journal of Lipid Research*, *51*(9), 2473-2488. https://doi.org/10.1194/jlr.R004119

Borchman, D., Lamba, O. P., & Yappert, M. C. (1993). Structural characterization of human lens membrane clear and cataractous lipid. *Experimental Eye Research*, *57*(2), 199-208. https://doi.org/10.1006/exer.1993.1115

Borchman, D., Stimmelmayr, R., & George, J. C. (2017). Whales, lifespan, phospholipids, and cataracts. *Journal of Lipid Research*, *58*(12), 2289-2298. https://doi.org/10.1194/jlr.M079368

Borchman, D., Tang, D., & Yappert, M. C. (1999). Lipid composition, membrane structure relationships in lens and muscle sarcoplasmic reticulum. *Biospectroscopy*, *5*(3), 151-167. https://doi.org/10.1002/(SICI)1520-6343(1999)5:3<151::AID-BSPY5>3.0.CO;2-D

Borchman, D., Yappert, M. C., & Afzal, M. (2004). Lens lipids and maximum lifespan. *Experimental Eye Research*, *79*(6), 761-768. https://doi.org/10.1016/j.exer.2004.04.004

Borchman, D., Yappert, M. C., & Herrell, P. (1991). Structural characterization of human lens membrane lipid by infrared spectroscopy. *Investigative Ophthalmology and Visual Sciences*, *32*(8), 236-248.

Borchman, D., Delamere, N. A., McCulley, L. A., & Paterson, C. A. (1989). Studies on the distribution of cholesterol, phospholipids and protein in the human and bovine lens. *Lens Eye Toxicity Research*, *6*(4), 703-724.

Borchman, D., Foulks, G. N., Yappert, M. C., & Ho, D. V. (2007). Temperature-induced conformational changes in human tear lipids hydrocarbon chains. *Biopolymers/Biospectroscopy*, *87*(2-3), 124-133.

Borchman, D., Ozaki, Y., Lamba, O. P., Byrdwell, W. C., & Yappert, M. C. (1996). Age and regional structural characterization of clear human lens lipid membranes by infrared and near-infrared Raman spectroscopes. *Biospectroscopy*, *2*, 113-123. https://doi.org/10.1002/(SICI)1520-6343(1996)2:2<113::AID-BSPY4>3.0.CO;2-A

Boveng, P. L., Bengtson, J. L., Cameron, M. F., Dahle, S. P., Logerwell, E. A., London, J. M., & Ziel, H. L. (2013). *Status review of the ribbon seal* (NOAA Technical Memorandum NMFS-AFSC-255). Washington, DC: U.S. Department of Commerce. 174 pp.

Boveng, P. L., Bengtson, J. L., Buckley, T. W., Cameron, M. F., Dahle, S. P., Kelly, B. P., . . . Williamson, N. J. (2009). *Status review of the spotted seal (*Phoca largha*)* (NOAA Technical Memorandum NMFS-AFSC-200). Washington, DC: U.S. Department of Commerce. 153 pp.

Broekhuyse, R. M., Kuhlmann, E. D., & Jap, P. H. K. (1979). Lens membranes. IX. Some characteristics of fiber membranes in relation to ageing and cataract formation. *Ophthalmic Research*, *11*(5-6), 423-428. https://doi.org/10.1159/000265045

Brzezińska-Slebodzińska, E. (2001). Fever induced oxidative stress: The effect on thyroid status and the 5'-monodeiodinase activity, protective role of selenium and vitamin E. *Journal of Physiological Pharmacology*, *52*(2), 275-284.

Byrdwell, W. C., Sato, H., Schwarz, A., Borchman, D., Yappert M. C., & Tang, D. (2002). ^{31}P-NMR quantification and monophasic solvent purification of human and bovine lens phospholipids. *Lipids*, *37*(11), 1087-1092. https://doi.org/10.1007/s11745-002-1004-1

Cameron, M. F., Frost, K. J., Ver Hoef, J. M., Breed, G. A., Whiting, A. V., Goodwin, J., & Boveng, P. L. (2018). Habitat selection and seasonal movements of young bearded seals (*Erignathus barbatus*) in the Bering Sea. *PLOS ONE*, *13*(2), e0192743. https://doi.org/10.1371/journal.pone.0192743

Cameron, M. F., Bengtson, J. L., Boveng, P. L., Jansen, J. K., Kelly, B. P., Dahle, S. P., . . . Wilder, J. M. (2010). *Status review of the bearded seal (*Erignathus barbatus*)* (NOAA Technical Memorandum NMFS-AFSC-211). Washington, DC: U.S. Department of Commerce.

Cantú-Medellín, N., Byrd, B., Hohn, A., Vázquez-Medina, J. P., & Zenteno-Savín, T. (2011). Differential antioxidant protection in tissues from marine mammals with distinct diving capacities: Shallow/short vs. deep/long divers. *Comparative Biochemistry and Physiology Part A: Molecular & Integrative Physiology*, *158*(4), 438-443. https://doi.org/10.1016/j.cbpa.2010.11.029

Coolitz, C. M., Saville, W. J., Renner, M. S., McBain, J. F., Reidarson, T. H., Schmitt, T. L., & Terrell, K. (2010). Risk factors associated with cataracts and lens luxations in captive pinnipeds in the United States and the Bahamas. *Journal of American Veterinary Medical Association*, *237*(4), 429-436. https://doi.org/10.2460/javma.237.4.429

Crawford, J. A., Quakenbush, L. T., & Citta, J. J. (2015). A comparison of ringed and bearded seal diet, condition and productivity between historical (1975-1984) and recent (2003-2012) periods in the Alaskan Bering and Chukchi Seas. *Progress in Oceanography*, *136*(SI), 133-150. https://doi.org/10.1016/j.pocean.2015.05.011

Davies, K. J. A. (1995). Oxidative stress: The paradox of aerobic life. *Biochemical Society Symposium*, *61*, 1-31. https://doi.org/10.1042/bss0610001

Deeley, J. M., Mitchell, T. W., Wei, X., Korth, J., Nealon, J. R., Blanksby, S. J., & Truscott, R. J. (2008). Human lens lipids differ markedly from those of commonly used experimental animals. *Biochimica Biophysica Acta*, *1781*(6-7), 288-298. https://doi.org/10.1016/j.bbalip.2008.04.002

Dickson, R. C. (1998). Sphingolipid functions in Saccharomyces cerevisiae: Comparison to mammals. *Annual Review of Biochemistry*, *67*, 27-48. https://doi.org/10.1146/annurev.biochem.67.1.27

Dioli, M., & Stimmelmayr, R. (1992). Ocular diseases. In H. J. Schwartz & M. Dioli (Eds.), *The one-humped camel in Eastern Africa: A pictorial guide to diseases, health care and management* (p. 223). Weikersheim, Germany: Verlag Josef Margraf Scientific Books.

Estrada, R., Puppato, A., Borchman, D., & Yappert, M. C. (2010). Re-evaluation of the phospholipid composition in membranes of adult human lenses by ^{31}P NMR and MALDI-MS. *Biochimica Biophysica Acta—Biomembranes*, *1798*(3), 303-311. https://doi.org/10.1016/j.bbamem.2009.11.008

El-Tookhy, O., & Tharwat, M. (2012). Clinical and ultrasonographic findings of some ocular affections in dromedary camels. *Journal of Camel Practice and Research*, *19*(2), 183-191.

Fay, F. H. (1982). Ecology and biology of the Pacific walrus, *Odobenus rosmarus divergens* Illiger. *North American Fauna*, *74*, 1-279. https://doi.org/10.3996/nafa.74.0001

Fay, F. H., & Burns, J. J. (1988). Maximal feeding depth of walruses. *Arctic*, *41*, 239-240. https://doi.org/10.14430/arctic1724

Ferguson-Yankey, S., Borchman, D., Taylor, K. G., DuPre, D. B., & Yappert, M. C. (2000). Conformational studies of sphingolipids by NMR spectroscopy. I. Dihydrosphingomyelin. *Biochimica Biophysica Acta*, *1467*(2), 307-325. https://doi.org/10.1016/S0005-2736(00)00228-5

Frost, K. J., & Lowry, L. F. (1980). Feeding of ribbon seals (*Phoca fasciata*) in the Bering Sea in spring. *Canadian Journal of Zoology*, *58*(9), 1601-1607. https://doi.org/10.1139/z80-219

Gatesy, J., Gesiler, J. H., Chang, J., Buell, C., Berta, A., Meredith, R. W., . . . McGowen, M. R. (2013). A phylogenetic blueprint for a modern whale. *Molecular Phylogenetics and Evolution*, *66*(2), 479-506. https://doi.org/10.1016/j.ympev.2012.10.012

George, J. C., Bada, J., Zeh, J., Scott, L., Brown, S., O'Hara, T. M., & Suydam, R. (1999). Age and growth estimates of bowhead whales (*Balaena mysticetus*) via aspartic acid racemization. *Canadian Journal of Zoology*, *77*(4), 571-580. https://doi.org/10.1016/j.ympev.2012.10.012

Gjertz, I., Kovacs, K. M., Lydersen, C., & Wiig, O. (2000). Movements and diving of bearded seal (*Erignathus barbatus*) mothers and pups during lactation and post-weaning. *Polar Biology*, *23*(8), 559-566. https://doi.org/10.1007/s003000000121

Greenwood, A. G. (1985). Prevalence of ocular anterior segment disease in captive pinnipeds. *Aquatic Mammals*, *11*(1), 13-15.

Hermes-Lima, M., Moreira, D. C., Rivera-Ingraham, G. A., Giraud-Billoud, M., Genaro-Mattos, T. C., & Campos, É. G. (2015). Preparation for oxidative stress under hypoxia and metabolic depression: Revisiting the proposal two decades later. *Free Radical Biology Medicine*, *89*, 1122-1143. https://doi.org/10.1016/j.freeradbiomed.2015.07.156

Herrero, A., Portero-Otin, M., Bellmunt, M. J., Pamplona, R., & Barja, G. (2001). Effect of the degree of fatty acid unsaturation of rat heart mitochondria on their rates of H_2O_2 production and lipid and protein oxidative damage. *Mechanisms of Ageing and Development*, *122*(4), 427-443. https://doi.org/10.1016/S0047-6374(01)00214-7

Higdon, J. W., Bininda-Emonds, O. R., Beck, R. M., & Ferguson, S. H. (2007). Phylogeny and divergence of the pinnipeds (Carnivora: Mammalia) assessed using a multigene dataset. *BMC Evolutionary Biology*, *7*, 216. https://doi.org/10.1186/1471-2148-7-216

Huang, L., Grami, V., Marrero, Y., Tang, D., Yappert, M. C., Rasi, V., & Borchman, D. (2005). Human lens phospholipid changes with age and cataract. *Investigative Ophthalmology and Visual Sciences*, *46*(5), 1682-1689. https://doi.org/10.1167/iovs.04-1155

Hubbard, R. C. (1970). The use of marine mammals in biomedical research. *Animal Models for Biomedical Research III, Proceedings of a Symposium, National Academy of Sciences, Washington, D.C.*, *3*, 133-146.

Hughes, J. R., Levchenko, V. A., Blanksby, S. J., Mitchell, T. W., Williams, A., & Truscott, R. J. (2015). No turnover in lens lipids for the entire human lifespan. *Elife*, *4*, e06003. https://doi.org/10.7554/eLife.06003

Hughes, J. R., Deeley, J. M., Blanksby, S. J., Leisch, F., Ellis, S. R., Truscott, R. J., & Mitchell, T. W. (2012). Instability of the cellular lipidome with age. *Age*, *34*(4), 935-947. https://doi.org/10.1007/s11357-011-9293-6

Kelly, B. P., & Wartzok, D. (1996). Ringed seal diving behavior in the breeding season. *Canadian Journal of Zoology*, *74*(8), 1547-1555. https://doi.org/10.1139/z96-169

Kimmich, R., & Peters, A. (1975). Solvation of oxygen in lecthin bilayers. *Chemistry and Physics of Lipids*, *14*(4), 350-362. https://doi.org/10.1016/0009-3084(75)90072-9

Kimmich, R., Peters, A., & Spohn, K. H. (1981). Solubility of oxygen in lecithin bilayers and other hydrocarbon lamellae as a probe for free volume and transport properties. *Journal of Membrane Science*, *9*(3), 313-336. https://doi.org/10.1016/S0376-7388(00)80272-0

Koretsky, I., Barnes, L., & Rahmat, S. (2016). Re-evaluation of morphological characters questions current views of pinniped origins. *Vestnik Zoologii*, *50*(4), 327-354. https://doi.org/10.1515/vzoo-2016-0040

Kóta, Z., Debreczeny, M., & Szalontai, B. (1999). Separable contributions of ordered and disordered lipid fatty acyl chain segments to $\tilde{\nu}CH_2$ bands in model and biological membranes: A Fourier transform infrared spectroscopic study. *Biospectroscopy*, *5*(3), 169-178. https://doi.org/10.1002/(SICI)1520-6343(1999)5:3<169::AID-BSPY6>3.0.CO;2-#

Krause, A. C. (1935). The chemistry of the lens: VI. Lipids. *Archives of Ophthalmology*, *13*(2), 187-190. https://doi.org/10.1001/archopht.1935.00840020047004

Li, S., Pang, J., Wilson, W. K., & Schroepfer, G. J., Jr. (1999). Sterol synthesis: Preparation and characterization of fluorinated and deuterated analogs of oxygenated derivatives of cholesterol. *Chemistry and Physics of Lipids*, *99*(1), 33-71. https://doi.org/10.1016/S0009-3084(99)00005-5

McLaren, I. A. (1958). The biology of the ringed seal (*Phoca hispida* Schreber) in the eastern Canadian Arctic. *Bulletin of the Fisheries Research Board of Canada* (No. 118).

Meneses, P., & Glonek, T. (1988). High resolution ^{31}P NMR of extracted phospholipids. *Journal of Lipid Research*, *29*(5), 679-689.

Muhr, P., Likussar, W., & Schubert-Zsilavecz, M. (1996). Structure investigation and proton and carbon-13 assignments of digitonin and cholesterol using multidimensional NMR techniques. *Magnetic Resonance Chemistry*, *34*(2), 137-142. https://doi.org/10.1002/(SICI)1097-458X(199602)34:2<137::AID-OM841>3.0.CO;2-Q

Nealon, J. R., Blanksby, S. J., Abbott, S. K. A., Hulbert, J., Mitchell, T. W., & Truscott, R. J. (2008). Phospholipid composition of the rat lens is independent of diet. *Experimental Eye Research*, *87*(6), 502-514. https://doi.org/10.1016/j.exer.2008.08.009

Noren, S. R., Jay, C. V., Burns, J. M., & Fischbach, A. S. (2015). Rapid maturation of the muscle biochemistry that supports diving in Pacific walruses (*Odobenus rosmarus divergens*). *Journal of Experimental Biology*, *218*(Pt 20), 3319-3329. https://doi.org/10.1242/jeb.125757

Oborina, E. M., & Yappert, M. C. (2003). Effect of sphingomyelin versus dipalmitoylphosphatidylcholine on the extent of lipid oxidation. *Chemistry and Physics of Lipids*, *123*(2), 223-232. https://doi.org/10.1016/S0009-3084(03)00003-3

Ortiz, R. M. (2001). Osmoregulation in marine mammals. *Journal of Experimental Biology*, *204*(11), 1831-1844.

Pamplona, R., Portero-Otin, M., Ruiz, C., Gredilla, C. R., & Herroro, A. (1999a). Double bond content of phospholipids and lipid peroxidation negatively correlate with maximum longevity in the heart of mammals. *Mechanisms of Ageing and Development*, *112*(3), 169-183. https://doi.org/10.1016/S0047-6374(99)00045-7

Pamplona, R., Portero-Otin, M., Requena, R. J., Thorpe, S. R., Herroro, A., & Barja, G. (1999b). A low degree of fatty acid unsaturation leads to lower lipid peroxidation and lipid oxidation-derived protein modification in heart mitochondria of the longevous pigeon than in the short-lived rat. *Mechanisms of Ageing and Development*, *106*(3), 283-296. https://doi.org/10.1016/S0047-6374(98)00121-3

Pamplona, R., Portero-Otin, M., Riba, D., Ruiz, C., Prat, J., Bellmunt, J. M., & Barja, G. (1998). Mitochondrial membrane peroxidizability index is inversely related to maximum life span in mammals. *Journal of Lipid Research*, *39*(10), 1989-1994.

Philo, L. M., Shotts, E. B., Jr., & George, J. C. (1993). Morbidity and mortality. In J. J. Burns, J. J. Montague, & C. J. Cowles (Eds.), *The bowhead whale* (Special Publication Number 2, pp. 275-307). Lawrence, KS: The Society for Marine Mammalogy.

Portero-Otin, M., Bellmunt, J. M., Ruiz, M. C., Barja, G., & Pamplona, R. (2001). Correlation of fatty acid unsaturation of the major liver mitochondria phospholipid classes in mammals to their maximum life span potential. *Lipids*, *36*(5), 491-498. https://doi.org/10.1007/s11745-001-0748-y

Power, G. G., & Stegall, H. (1970). Solubility of gases in human red blood cell ghosts. *Journal of Applied Physiology*, *29*(2), 145-149. https://doi.org/10.1152/jappl.1970.29.2.145

Quakenbush, L., Citta, J., & Crawford, J. (2009). *Biology of the spotted seal (*Phoca largha*) in Alaska from 1962 to 2008* (Report to the National Marine Fisheries Service). Retrieved from www.adfg.alaska.gov/static-f/research/programs/marinemammals/pdfs/biology_spotted_seal.pdf

Rivera-Ingraham, G. A., & Lignot, J-H. (2017). Osmoregulation, bioenergetics and oxidative stress in coastal marine invertebrates: Raising the questions for future research. *Journal of Experimental Biology*, *220*, 1749-1760. https://doi.org/10.1242/jeb.135624

Rivera-Ingraham, G. A., Nommick, A., Blondeau-Bidet, E., Ladurner, P., & Lignot, J-H. (2016). Salinity stress from the perspective of the energy-redox axis: Lessons from a marine intertidal flatworm. *Redox Biology*, *10*, 53-64. https://doi.org/10.1016/j.redox.2016.09.012

Sawan, S. P., James, T. L., Gruenke, L. D., & Craig, J. C. (1979). Proton NMR assignments for cholesterol: Use of deuterium NMR as an assignment aid. *Journal of Magnetic Resonance*, *35*(3), 409-413. https://doi.org/10.1016/0022-2364(79)90063-5

Schmidt-Nielsen, K., Schmidt-Nielsen, B., Jarnum, S. A., & Haupt, T. R. (1956). Body temperature of the camel and its relation to water economy. *American Journal of Physiology–Legacy Content*, *188*(1), 103-112. https://doi.org/10.1152/ajplegacy.1956.188.1.103

Schmidt-Nielsen, K., Crawford, E. C., Jr., Newsome, A. E., Rawson, K. S., & Hammel, H. T. (1967). Metabolic rate of camels: Effect of body temperature and dehydration. *American Journal of Physiology–Legacy Content*, *212*(2), 341-346. https://doi.org/10.1152/ajplegacy.1967.212.2.341

Seim, I., Ma, S., Zhou, X., Gerashchenko, M. V., Lee, S-G., Suydam, R., & Gladyshev, V. N. (2014). The transcriptome of the bowhead whale (*Balaena mysticetus*) reveals adaptations of the longest-lived mammal. *Aging*, *6*(10), 879-899. https://doi.org/10.18632/aging.100699

Sheffield, G., & Grebmeier, J. M. (2009). Pacific walrus (*Odobenus rosmarus divergens*): Differential prey digestion and diet. *Marine Mammal Science*, *25*(4), 761-777. https://doi.org/10.1111/j.1748-7692.2009.00316.x

Smotkin, E. S., Moy, F. T., & Plachy, W. Z. (1991). Dioxygen solubility in aqueous phosphatidylcholine dispersions. *Biochimica and Biophysica Acta*, *1096*(1), 33-38. https://doi.org/10.1016/0005-2736(91)90265-A

Sparling, M. L., Zidovetzki, R., Muller, L., & Chan, S. I. (1989). Analysis of membrane lipids by 500 MHz ^{1}H NMR. *Analytical Biochemistry*, *178*(1), 67-76. https://doi.org/10.1016/0003-2697(89)90358-8

Stimmelmayr, R. (2015). *Health assessment of subsistence harvested Bering-Chukchi-Beaufort Seas bowhead whales (*Balaena mysticetus*): An overview* (Science Paper SC/66a/E/8). Paper presented to the International Whaling Commission (IWC), Bled, Slovenia.

Subczynski, W. K., & Hyde, J. S. (1983). Concentration of oxygen in lipid bilayers using a spin-label method. *Biophysical Journal*, *41*(3), 283-286. https://doi.org/10.1016/S0006-3495(83)84439-7

Talbot, C. M., Vorobyov, I., Borchman, D., Taylor, K. G., DuPre, D. B., & Yappert, M. C. (2000). Conformational studies of sphingolipids by NMR spectroscopy. II. Sphingomyelin. *Biochimica and Biophysica Acta*, *1467*(2), 326-337. https://doi.org/10.1016/S0005-2736(00)00229-7

Vanderkooi, J. M., Wright, W. W., & Erecinska, M. (1990). Oxygen gradients in mitochondria examined with delayed luminescence from excited-state triplet probes. *Biochemistry*, *29*(22), 5332-5338. https://doi.org/10.1021/bi00474a018

Vazquez-Medina, J. P., Zenteno-Savín, T., Elsner, R., & Ortiz, R. M. (2012). Coping with physiological oxidative stress: A review of antioxidant strategies in seals. *Journal of Comparative Physiology B*, *182*(6), 741-750. https://doi.org/10.1007/s00360-012-0652-0

Wu, H., Guang, X., Al-Fageeh, M. B., Cao, J., Pan, S., Zhou, H., . . . Wang, J. (2014). Camelid genomes reveal evolution and adaptation to desert environments. *Nature Communications*, *21*(5), 5188. https://doi.org/10.1038/ncomms6188

Xu, S., Yang, Y., Zhou, X., Xu, J., Zhou, K., & Yang, G. (2013). Adaptive evolution of the osmoregulation-related genes in cetaceans during secondary aquatic adaptation. *BMC Evolutionary Biology*, *13*, 189. https://doi.org/10.1186/1471-2148-13-189

Yim, H. S., Cho, Y. S., Guang, X., Kang, S. G., Jeong, J. Y., Cha, S. S., & Lee, J. H. (2014). Minke whale genome and aquatic adaptation in cetaceans. *Nature Genetics*, *46*(1), 88-92. https://doi.org/10.1038/ng.2835

Young, K. (2013). *Lipid studies in breath-hold diving mammals and obese, pre-diabetic mice* (PhD thesis). Baylor University, Waco, TX. 144 pp. Retrieved from https://baylor-ir.tdl.org/baylor-ir/bitstream/handle/2104/8925/kathy_young_phd.pdf?sequence=1

Zeh, J., Craig, G. J., Botta, O., & Zauscher, M. (2013). Age and growth estimates of bowhead whales (*Balaena mysticetus*) via aspartic acid racemization. *Marine Mammal Science*, *29*(3), 424-445.